

## Decorating Metal Oxide Surfaces with Fluorescent Chlorosulfonated Corroles

Carl M. Blumenfeld,<sup>†,‡</sup> Robert H. Grubbs,<sup>‡</sup> Rex A. Moats,<sup>§</sup> Harry B. Gray,<sup>\*,†,‡</sup> and Karn Sorasaene<sup>\*,†,‡,§</sup><sup>†</sup>Beckman Institute and <sup>‡</sup>Department of Chemistry, California Institute of Technology, Pasadena, California 91125, United States<sup>§</sup>Translational Biomedical Imaging Center, Department of Radiology, The Saban Research Institute, Children's Hospital Los Angeles, University of Southern California, Los Angeles, California 90027, United States

## Supporting Information

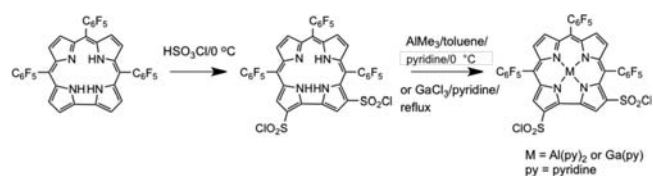
**ABSTRACT:** We have prepared 2,17-bis(chlorosulfonyl)-5,10,15-tris(pentafluorophenyl)corrole (**1**), 2,17-bis(chlorosulfonyl)-5,10,15-tris(pentafluorophenyl)corrolatoaluminum(III) (**1-Al**), and 2,17-bis(chlorosulfonyl)-5,10,15-tris(pentafluorophenyl)corrolatogallium(III) (**1-Ga**). The metal complexes **1-Al** and **1-Ga** were isolated and characterized by electronic absorption and NMR spectroscopies, as well as by mass spectrometry. Relative emission quantum yields for **1**, **1-Al**, and **1-Ga**, determined in toluene, are 0.094, 0.127, and 0.099, respectively. Reactions between **1**, **1-Al**, and **1-Ga** and TiO<sub>2</sub> nanoparticles (NPs) result in corrole–TiO<sub>2</sub> NP conjugates. The functionalized NP surfaces were investigated by solid-state Fourier transform infrared and X-ray photoelectron spectroscopies and by confocal fluorescence imaging. The fluorescence images for **1-Al**–TiO<sub>2</sub> and **1-Ga**–TiO<sub>2</sub> suggest a promising application of these NP conjugates as contrast agents for noninvasive optical imaging.

In recent years, molecular imaging has attracted much attention in the medical field for both the diagnosis of and intervention against disease.<sup>1</sup> Although a myriad of imaging modalities have enormously contributed to biomedical research,<sup>2</sup> probe development is still a very high priority.<sup>3</sup> Historically, small-molecule and biomolecule contrast agents have been prepared and studied in the context of their corresponding imaging modalities.<sup>4</sup> More recently, nanomaterial probes, such as quantum dots and iron oxide nanoparticles (NPs), have been developed and employed in molecular imaging.<sup>5</sup> Studies of and interests in these nanomaterials as contrast agents also suggest the possibility of extensive probe development in biomedical imaging. In this study, we focus on the use of versatile fluorescent small molecules, namely, corroles, as potential contrast agents in optical imaging. Corroles are facilely modified using multiple approaches including both aromatic and asymmetric substitution at the *meso*-aryl position as well as modification at the  $\beta$ -pyrrolic positions, making these tetrapyrrolic macrocycles strong candidates for readily tunable imaging systems.<sup>6</sup>

Recently, there has been much effort in developing these macrocycles as optical dyes because of their unique fluorescence properties.<sup>7</sup> Previous imaging studies employing corroles have only been pursued with noncovalent assemblies between the macrocycle and proteins.<sup>8</sup> For the first time, we report the use of

corroles as synthons for optical imaging agents with applications involving covalently bound NPs. The preparation of the parent free-base macrocycle 2,17-bis(chlorosulfonyl)-5,10,15-tris(pentafluorophenyl)corrole (**1**) has been reported;<sup>9</sup> however, before our work, the metalated species had not been prepared. Here we report the preparation and characterization of **1**, 2,17-bis(chlorosulfonyl)-5,10,15-tris(pentafluorophenyl)corrolatoaluminum(III) (**1-Al**), and 2,17-bis(chlorosulfonyl)-5,10,15-tris(pentafluorophenyl)corrolatogallium(III) (**1-Ga**). In addition, spectroscopic and photophysical studies, which serve as a fundamental platform for further development of these bis-chlorosulfonated corroles as building blocks for optical contrast agents, will be addressed. We will also discuss surface modification reactions by which **1**, **1-Al**, and **1-Ga** can be covalently coupled to TiO<sub>2</sub> NP surfaces as well as surface characterization of the TiO<sub>2</sub>–corrole nanoconjugates.

Corrole **1** has been prepared according to the literature.<sup>9</sup> Metal-insertion reactions of **1** with AlMe<sub>3</sub> in a toluene/pyridine mixture at 0 °C and GaCl<sub>3</sub> in pyridine at reflux afford the products **1-Al** (26% yield) and **1-Ga** (39% yield), respectively (Scheme 1). Both **1-Al** and **1-Ga** were isolated by solvent

Scheme 1. Preparation of Metalated **1**

extraction and obtained as green solids after evaporation to dryness. The metalated products were further purified by acetone/methylene chloride assisted filtration followed by the removal of solvents in vacuo.

Electronic absorption spectra for **1**, **1-Al**, and **1-Ga** obtained in degassed toluene solutions reveal the signature Soret and Q bands for these tetrapyrrolic macrocycles (Figure 1). The electronic absorption data for the chlorosulfonated corroles are also given in Table 1. Compared to the parent compound **1**, each of the metalated chlorosulfonated corroles **1-Al** and **1-Ga** exhibits a sharper Soret band with a vibronic shoulder to the left (characteristic of the metalated species) that is blue-shifted at

Received: February 16, 2013

Published: April 23, 2013

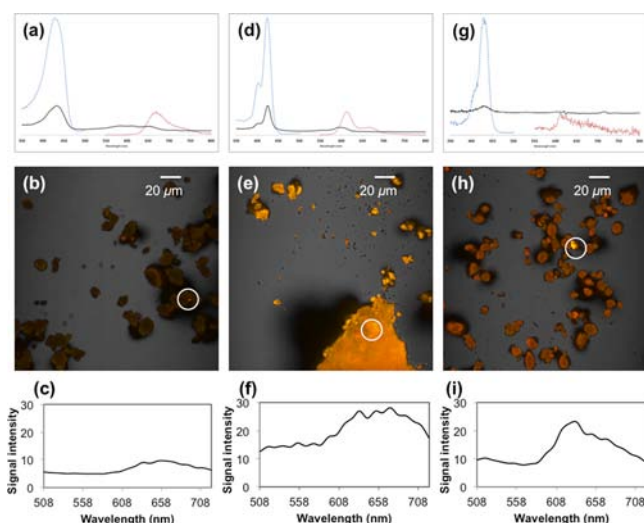


**Figure 1.** First row: Absorption (black), excitation (blue), and emission (red) spectra for **1** (a), **1-Al** (d), and **1-Ga** (g). Second row: Superimposed confocal fluorescence pseudocolor and bright-field images for **1-TiO<sub>2</sub>** (b), **1-Al-TiO<sub>2</sub>** (e), and **1-Ga-TiO<sub>2</sub>** (h). Third row: Fluorescence profiles of **1-TiO<sub>2</sub>** (c), **1-Al-TiO<sub>2</sub>** (f), and **1-Ga-TiO<sub>2</sub>** (i) aggregates with  $\lambda_{\text{ex}} = 405$  nm. The white circles represent the selected areas from which the corresponding spectral profiles were derived.

**Table 1. Electronic Spectroscopic Data for Chlorosulfonated Corroles **1**, **1-Al**, and **1-Ga** in Toluene Solutions**

corrole	electronic absorption <sup>a</sup>		fluorescence <sup>a</sup>		
	$\lambda_{\text{max}}^b$ (nm)		$\lambda_{\text{ex}}$ (nm)	$\lambda_{\text{em}}$ (nm)	$\phi_{\text{em}}^c$
<b>1</b>	430 (S), 580 (Q)		426	670	0.094
<b>1-Al</b>	424 (S), 592 (Q)		420	611	0.127
<b>1-Ga</b>	426 (S), 588 (Q)		427	609	0.099

<sup>a</sup>The measurements were performed in degassed toluene. <sup>b</sup>The maximum absorption wavelengths are reported for both Soret (S) and Q bands. <sup>c</sup>The relative emission quantum yields were determined using tetraphenylporphyrin as the standard.

424 and 426 nm, respectively, as shown in Figure 1. The Q bands for both **1-Al** and **1-Ga** are also narrower and are observed at 592 and 588 nm, respectively. This could be further explained by the presence of a single absorbing species for the metalated corroles, while the nonmetalated corrole could exhibit two tautomeric forms.<sup>10g,h</sup>

Similar to other pentafluorophenyl corroles, **1**, **1-Al**, and **1-Ga** exhibit bright fluorescence, particularly **1-Al**, with a large Stokes shift.<sup>10</sup> Excitation into the Soret or Q bands results in an emission spectral profile similar to that with  $\lambda_{\text{em}}$  observed around 600–670 nm (Figure 1) accompanied by a vibronic band to the red of the major emission peak for the three corroles. The excitation and emission wavelengths observed are set out in Table 1. We note that chlorosulfonated metallo-corroles **1-Al** and **1-Ga** follow the expected trend for fluorescence in which  $\lambda_{\text{em}}$  (611 nm) for the slightly more electropositive **1-Al** is more red-shifted compared to  $\lambda_{\text{em}}$  (609 nm) for **1-Ga** because of a destabilized highest occupied molecular orbital.<sup>11</sup> The quantum yield measurements, relative to tetraphenylporphyrin,<sup>12</sup> with  $\lambda_{\text{ex}} = 355$  nm for **1**, **1-Al**, and **1-Ga** reveal  $\phi_{\text{em}} = 0.094$ , 0.127, and 0.099, respectively. As expected, the aluminum chlorosulfonated corrole exhibits the highest relative quantum yield, consistent with the previously reported relative quantum yield for the nonsulfonated

aluminum(III) corrole.<sup>10b,c</sup> The  $\phi_{\text{em}}$  trend for all three chlorosulfonated corroles is comparable to that reported elsewhere for nonsulfonated compounds.<sup>10a–c</sup>

On the basis of modification of the chlorosulfonyl group with alcohols producing sulfonic esters,<sup>13</sup> we report the covalent modification of a chlorosulfonyl group with a new hydroxyl platform, namely, TiO<sub>2</sub> NPs with hydroxylated surfaces, as an example of the versatility of chlorosulfonated corroles and their potential uses in optical imaging applications. Corrole coupling to TiO<sub>2</sub> NPs was performed following enhanced hydroxylation of the surface using H<sub>2</sub>O<sub>2</sub>. The NPs bearing the hydroxylated surfaces were mixed with pyridine solutions of corrole and heated to reflux. After repeated washing with copious amounts of CH<sub>2</sub>Cl<sub>2</sub>, acetone, and water and drying under high vacuum, green powders were obtained. The electronic absorption spectra (see the Supporting Information, SI) of the colloidal suspensions of **1-TiO<sub>2</sub>**, **1-Al-TiO<sub>2</sub>**, and **1-Ga-TiO<sub>2</sub>** nanoconjugates in phosphate-buffered saline (pH 7.4) reveal maximum absorptions centered around 425 and 600 nm for the Soret and Q bands, respectively (Table 2). These peak maxima are in agreement with

**Table 2. Electronic Absorption, Vibrational, and X-ray Photoelectron Spectroscopic Data for Corrole-TiO<sub>2</sub> Nanoconjugates **1-TiO<sub>2</sub>**, **1-Al-TiO<sub>2</sub>**, and **1-Ga-TiO<sub>2</sub>****

conjugate	electronic absorption		SO <sub>2</sub> vibrational frequency (cm <sup>-1</sup> )		F(1s) binding energy (eV)
	$\lambda_{\text{max}}$ (nm)		sym	asym	
<b>1-TiO<sub>2</sub></b>	415, 430 (S), 591, 621 (Q)		1153	1410	691
<b>1-Al-TiO<sub>2</sub></b>	427 (S), 576, 610 (Q)		1244	1431	690
<b>1-Ga-TiO<sub>2</sub></b>	423 (S), 589, 610 (Q)		1160	1450	688

the spectroscopic properties of the corresponding molecular corrole (Table 1). We also note that the Soret band splitting for **1-TiO<sub>2</sub>** is similar to the splitting observed for its amphiphilic molecular counterpart 2,17-disulfonato-5,10,15-tris-(pentafluorophenyl)corrole in an aqueous solution at physiological pH, supporting the presence of the sulfonate linkage on the corrole anchored to TiO<sub>2</sub> surfaces. The splitting pattern, however, is not observed for the metalloconjugates **1-Al-TiO<sub>2</sub>** and **1-Ga-TiO<sub>2</sub>**, due to the presence of metal bound to deprotonated nitrogen atoms.<sup>10b–d,h</sup>

Characterization of the fine green powder of **1-TiO<sub>2</sub>**, **1-Al-TiO<sub>2</sub>**, and **1-Ga-TiO<sub>2</sub>** with Fourier transform infrared spectroscopy reveals vibrational absorption bands around 1150–1250 cm<sup>-1</sup> assigned to the symmetric stretching of SO<sub>2</sub> groups as well as those around 1400–1450 cm<sup>-1</sup> assigned to asymmetric stretching of SO<sub>2</sub> groups of covalent sulfonates.<sup>14</sup> The presence of these vibrational signatures suggests that the corroles are covalently attached to the surface of TiO<sub>2</sub> through a sulfonate linkage. The vibrational frequencies for these TiO<sub>2</sub>-corrole nanoconjugates are listed in Table 2. X-ray photoelectron spectroscopy was performed to study the elemental presence of the surface of the NP conjugates (Table 2). High-resolution scans for the spectra (see the SI) of the conjugates revealed F(1s) binding energy peaks between 688 and 691 eV,<sup>15</sup> suggesting the presence of corresponding (pentafluorophenyl)corroles attached to the TiO<sub>2</sub> surface.

Confocal fluorescence microscopy images of aggregates of the nanoconjugates **1**-TiO<sub>2</sub>, **1-Al**-TiO<sub>2</sub>, and **1-Ga**-TiO<sub>2</sub> in the solid state (Figure 1) were taken with the samples illuminated at  $\lambda_{\text{ex}} = 405$  nm and  $\lambda_{\text{em}}$  recorded from 508 to 722 nm. The images for **1-Al**-TiO<sub>2</sub> and **1-Ga**-TiO<sub>2</sub> (Figure 1e,h) exhibit fluorescence areas on the NPs compared to the relatively darker image for **1**-TiO<sub>2</sub>. The fluorescence signals observed with various intensities across the TiO<sub>2</sub> samples for **1-Al**-TiO<sub>2</sub> and **1-Ga**-TiO<sub>2</sub> also suggest that the TiO<sub>2</sub> surfaces are not evenly functionalized because of material aggregation. More detailed studies of the quenching of the fluorescence of **1**-TiO<sub>2</sub> are underway in our laboratories. Upon closer inspection, however, of selected fluorescence areas (white circles) on all three images, spectral profiles representing the nanoconjugates **1**-TiO<sub>2</sub>, **1-Al**-TiO<sub>2</sub>, and **1-Ga**-TiO<sub>2</sub> were obtained (Figure 1c,f,i). We note that these spectral profiles and fluorescence signal intensities are in agreement with the fluorescence spectra (Figures 1a,d,g) obtained from the molecular corroles **1**, **1-Al**, and **1-Ga**.

In summary, we have prepared TiO<sub>2</sub> nanoconjugates whose surfaces were covalently modified with fluorescent chlorosulfonated corroles through sulfonic ester formation. The nanoconjugate **1-Al**-TiO<sub>2</sub> exhibits the most intense fluorescence based on the spectral plot obtained from confocal fluorescence microscopy images. This finding is in line with the fluorescence behavior (high relative  $\phi_{\text{em}}$ ) of **1-Al**. Further biological and imaging experiments involving these fluorescent nanoconjugates as potential contrast agents for optical imaging are underway in our laboratories.

## ■ ASSOCIATED CONTENT

### ■ Supporting Information

Synthetic procedures, experimental details for characterization and imaging, and spectroscopic and mass spectrometric information. This material is available free of charge via the Internet at <http://pubs.acs.org>.

## ■ AUTHOR INFORMATION

### ■ Corresponding Author

\*E-mail: [hbg@its.caltech.edu](mailto:hbg@its.caltech.edu) (H.B.G.), [ksorasaene@chla.usc.edu](mailto:ksorasaene@chla.usc.edu) (K.S.).

### ■ Notes

The authors declare no competing financial interest.

## ■ ACKNOWLEDGMENTS

We thank the CHLA Radiology Endowment Fund, Sanofi, and Doheny Eye Institute for financial support. We thank Esteban Fernandez, George Rossman, Bruce Brunswick, Zeev Gross, and Michael Lichterman for their help and discussion on this work. We thank Mona Shahgholi (CCE Division Multiuser Mass Spectrometry Lab at Caltech) for her help with electrospray ionization mass spectrometry experiments.

## ■ REFERENCES

- (1) (a) Tempany, C. M.; McNeil, B. J. *JAMA* **2001**, *285*, 562. (b) Herschman, H. R. *Science* **2003**, *302*, 605. (c) Weissleder, R.; Pittet, M. J. *Nature* **2008**, *452*, 580. (d) Mura, S.; Couvreur, P. *Adv. Drug Delivery Rev.* **2012**, *64*, 1394.
- (2) (a) Ntziachristos, V.; Ripoll, J.; Wang, L. V.; Weissleder, R. *Nat. Biotechnol.* **2005**, *23*, 313. (b) Borsook, D.; Becerra, L.; Hargreaves, R. *Nat. Rev. Drug Discovery* **2006**, *5*, 411.
- (3) Willmann, J. K.; Van Bruggen, N.; Dinkelborg, L. M.; Gambhir, S. *Nat. Rev. Drug Discovery* **2008**, *7*, 591.

- (4) Winter, P. M.; Caruthers, S. D.; Kassner, A.; Harris, T. D.; Chinen, L. K.; Allen, J. S.; Lacy, E. K.; Zhang, H.; Robertson, J. D.; Wickline, S. A.; Lanza, G. M. *Cancer Res.* **2003**, *63*, 5838.

- (5) (a) Endres, P. J.; Paunesku, T.; Vogt, S.; Meade, T. J.; Woloschak, G. E. *J. Am. Chem. Soc.* **2007**, *129*, 15760. (b) Xie, J. *Inorg. Chem.* **2008**, *47*, 5564. (c) Zhang, W.; Zhou, X.; Zhong, X. *Inorg. Chem.* **2012**, *51*, 3579. (d) Rodriguez-Liviano, S.; Becerro, A. I.; Alcántara, D.; Grazú, V.; De la Fuente, J. M.; Ocaña, M. *Inorg. Chem.* **2013**, *52*, 647.

- (6) (a) Gross, Z.; Galili, N.; Saltsman, I. *Angew. Chem., Int. Ed.* **1999**, *38*, 1427. (b) Sankar, J.; Anand, V. G.; Venkatraman, S.; Rath, H.; Chandrashekar, T. K. *Org. Lett.* **2002**, *4*, 4233. (c) Ngo, T. H.; Puntoriero, F.; Nastasi, F.; Robeyns, K.; Van Meervelt, L.; Campagna, S.; Dehaen, W.; Maes, W. *Chem.—Eur. J.* **2010**, *16*, 5691.

- (7) (a) Mohammed, A.; Gray, H. B.; Weaver, J. J.; Sorasaene, K.; Gross, Z. *Bioconjugate Chem.* **2004**, *15*, 738. (b) Li, C.-Y.; Zhang, X.-B.; Han, Z.-X.; Akermark, B.; Sun, L.; Shen, G.-L.; Yu, R.-Q. *Analyst* **2006**, *131*, 388.

- (8) (a) Agadjanian, H.; Weaver, J. J.; Mohammed, A.; Rentsendorj, A.; Bass, S.; Kim, J.; Dmochowski, I. J.; Margalit, R.; Gray, H. B.; Gross, Z.; Medina-Kauwe, L. K. *Pharm. Res.* **2006**, *23*, 367. (b) Agadjanian, H.; Ma, J.; Rentsendorj, A.; Valluripalli, V.; Hwang, J. Y.; Mohammed, A.; Farkas, D. L.; Gray, H. B.; Gross, Z.; Medina-Kauwe, L. K. *Proc. Natl. Acad. Sci. U.S.A.* **2009**, *106*, 6105.

- (9) (a) Mohammed, A.; Goldberg, I.; Gross, Z. *Org. Lett.* **2001**, *3*, 3443. (b) Saltsman, I.; Mohammed, A.; Goldberg, I.; Tkachecko, E.; Botoshansky, M.; Gross, Z. *J. Am. Chem. Soc.* **2002**, *124*, 7411.

- (10) (a) Bendix, J.; Dmochowski, I. J.; Gray, H. B.; Mohammed, A.; Simkhovich, L.; Gross, Z. *Angew. Chem., Int. Ed.* **2000**, *112*, 4214. (b) Mohammed, A.; Gross, Z. *J. Inorg. Biochem.* **2002**, *88*, 305.

- (c) Weaver, J. J.; Sorasaene, K.; Sheikh, M.; Goldschmidt, R.; Tkachenko, E.; Gross, Z.; Gray, H. B. *J. Porphyrins Phthalocyanines* **2004**, *08*, 76. (d) Sorasaene, K.; Taqavi, P.; Henling, L. M.; Gray, H. B.; Tkachenko, E.; Mohammed, A.; Gross, Z. *J. Porphyrins Phthalocyanines* **2007**, *11*, 189. (e) Kowalska, D.; Liu, X.; Tripathy, U.; Mohammed, A.; Gross, Z.; Hirayama, S.; Steer, R. P. *Inorg. Chem.* **2009**, *48*, 2670.

- (f) Yang, Y.; Jones, D.; Von Haimberger, T.; Linke, M.; Wagnert, L.; Berg, A.; Levanon, H.; Zacarias, A.; Mohammed, A.; Gross, Z.; Heyne, K. *J. Phys. Chem. A* **2012**, *116*, 1023. (g) Ivanova, Y. B.; Savva, V. A.; Mamardashvili, N. Z.; Starukhin, A. S.; Ngo, T. H.; Dehaen, W.; Maes, W.; Kruk, M. M. *J. Phys. Chem. A* **2012**, *116*, 10683. (h) Kruk, M.; Ngo, T. H.; Savva, V.; Starukhin, A.; Dehaen, W.; Maes, W. *J. Phys. Chem. A* **2012**, *116*, 10704. (i) Kruk, M.; Ngo, T. H.; Verstappen, P.; Starukhin, A.; Hofkens, J.; Dehaen, W.; Maes, W. *J. Phys. Chem. A* **2012**, *116*, 10695.

- (11) (a) Hush, N.; Dyke, J. *Dalton Trans.* **1974**, 395. (b) Ghosh, A.; Wondimagegn, T.; Parusel, A. B. *J. Am. Chem. Soc.* **2000**, *122*, 5100.

- (12) Seybold, P. G.; Gouterman, M. *J. Mol. Spectrosc.* **1969**, *31*, 1.

- (13) Reynolds, D.; Kenyon, W. *J. Am. Chem. Soc.* **1950**, *72*, 1584.

- (14) Socrates, G. *Infrared and Raman Characteristic Group Frequencies: Table and Charts*; John Wiley & Sons: Chichester, U.K., 2001; p 218.

- (15) Barron, A. R., Ed. *Physical Methods in Chemistry and Nano Science*; Connexions: Houston, TX, 2012; p 365.

## ■ NOTE ADDED AFTER ASAP PUBLICATION

Due to a production error, this paper was published ASAP on April 23, 2013, with minor errors in the caption for Figure 1. The corrected version was reposted on April 24, 2013.